Precision Engineering 51 (2018) 338–347

Contents lists available at ScienceDirect

Precision Engineering

journal homepage: www.elsevier.com/locate/precision

An improved signal determination method on machined surface topography

Jingjing Sun[a,b], Zhanjie Song[a], Gaiyun He[b,*], Yicun Sang[b]

[a] School of Mathematics, Tianjin University, Tianjin 300354, China
[b] Key Laboratory of Mechanism Theory and Equipment Design of Ministry of Education, Tianjin University, Tianjin 300354, China

ARTICLE INFO

Keywords:
Wavelet denoising
Ensemble empirical mode decomposition
Transfer function
Compensation

ABSTRACT

The characteristic signals of the machined surface are a mixture of actual signals and noise. It is feasible to make the features distinct through wavelet denoising. However, some of the deterministic signals may be lost with noise removed resulting in the loss of energy which make it difficult to judge the real components of the surface. An improved signal determination method —— wavelet denoising with compensation of the loss (WDCL) is proposed in this paper. The compensation method uses ensemble empirical mode decomposition (EEMD) and transfer function in which instantaneous frequency is calculated by Hilbert transform (HT). The coefficients of the transfer function are adjusted by improving the passing rate of the deterministic signals and lowering the passing rate of noise. The result shows that the WDCL can enhance the resolution of the real signals and reduce noise further.

1. Introduction

Machined surface feature is composed of dissimilar components varying in scale or frequency, these components contain useful information to trace errors of the machine. A variety of errors will be reflected in the surface topography of the workpiece during the machining process. So all the effective components of the surface topography are important for identifying the error source by feature extraction so as to improve the machining accuracy further [1–3]. However, it is often immersed in heavy noise. The noise could be generated by aperiodic stochastic vibration which is caused by random factors during the cutting process and distributed throughout the entire frequency domain. So it is necessary to carry out full frequency-domain noise reduction first. Denoising process is usually done in the frequency domain. Many filters could be used for denoising such like the 2RC, Gaussian, B-spline and digital filters [4–6] etc. They are essentially various signal analysis techniques. However, in terms of noise reduction, when the noise spectrum and signal spectrum overlap, the filters above not only lose certain real frequency information, but also can not achieve good noise reduction effect in the reserved frequency domain. On the other hand, the time–frequency analysis methods have been widely used. In the early studies, Fourier analysis was the dominant signal analysis tool for denoising. But there are some crucial restrictions of the Fourier transform [7]: the signals to be analysed must be periodic or stationary, otherwise it would make little physical sense. Moreover, it can only get frequency information of main component losing the spatial information at the same time. In fact, the machined surface features are usually non-stationary and non-linear, thus Fourier transform cannot get the desired results to deal with surface quality characteristics. In the later works, wavelet transform has become popular which can get both frequency and spatial information of surface topography. It can also decompose the different frequency components in the signal to a non-overlapping frequency band and carry out noise reduction in the entire frequency domain. This is another aspect which is superior to the traditional denoising methods based on filtering. It has been widely used in mechanical surface diagnosis [8]. One of the most widely used methods was wavelet threshold denoising method. Donoho and Johnstone [9] proposed a uniform threshold method in 1994. Cai and Silverman [10] proposed a denoising method based on neighbouring coefficients (NeighCoeff) in 1999. However, the wavelet denoising method still have some inevitable deficiencies [11], including the interference terms, border distortion and energy leakage. In fact, almost all the denoising methods have energy leakage problems.

Recently, another time–frequency analysis method named Hilbert–Huang transform (HHT) [12–15] has become increasingly popular. It is a combination of empirical mode decomposition (EMD) and Hilbert transform (HT). EMD is a time adaptive decomposition operation which can decompose the signal into a set of complete and almost orthogonal components named intrinsic mode function (IMF) [7], which are almost monocomponent. Zhang et al. [16] combined wavelet reconstruction with EMD. However, one of the major drawbacks of EMD is the mode mixing problem. To alleviate the problem, ensemble empirical mode decomposition (EEMD), an improved method of EMD, was presented by Wu and Huang [17] in 2011. The EEMD

* Corresponding author.
E-mail address: hegaiyun@tju.edu.cn (G. He).

http://dx.doi.org/10.1016/j.precisioneng.2017.09.004
Received 8 March 2017; Received in revised form 30 August 2017; Accepted 5 September 2017
Available online 07 September 2017
0141-6359/

method can eliminate the mode mixing problem in all cases automatically. It has been developed and widely applied in fault diagnosis of rotating machinery recently [18,19]. By using the Hilbert transform on IMFs, the instantaneous frequency, phase and amplitude of signals can be obtained. In control systems, error compensation is often performed with the help of transfer function [20,21]. For wavelet denoising process, the transfer function can be obtained by inputting and outputting data with which the energy loss can be compensated to some extent. In the seismic data processing, the problem of energy loss also exist. There are many time–frequency analysis methods based on energy compensation [22–24]. Given that the high frequency data is easy to lose, most of the compensation methods are only used for high frequency compensation.

Almost all the traditional noise reduction methods have the problem of energy loss. In order to effectively eliminate noise while retaining the true component of machined surface feature, an improved signal determination method —— wavelet denoising with compensation of the loss (WDCL) is proposed in this paper. It utilizes the excellent properties of wavelet in signal denoising throughout the entire frequency domain, combined with good decomposition ability of EEMD and the compensation roll of transfer function of each IMF. The result shows that the WDCL method could not only denoise the entire frequency component, but also perform energy compensation after noise reduction which achieves a better denoising effect than traditional denoising method.

2. Wavelet transform and Hilbert–Huang transform theory

2.1. Wavelet transform theory

Wavelet transform is a mathematical transformation method, and it can decompose a given signal into different levels using wavelet bases. The base function of wavelet transform is given by:

$$\psi_{s,\tau}(t) = \frac{1}{\sqrt{s}}\psi\left(\frac{t-\tau}{s}\right) \quad s, \tau \in Z \tag{1}$$

where ψ is mother wavelet, all the wavelet bases $\psi_{s,\tau}$ are formed by translating and stretching mother wavelet with factor s and τ. The discrete form of wavelet transform of signal $f(x)$ at scale j can be written as:

$$\mathrm{Wf}[j, i] = \sum_{n=1}^{N} f[n]\psi[n-i] \tag{2}$$

where $j = 1, 2, \ldots, N$, N is the total discrete steps.

In addition to the wavelet base function, another base function named scale-function is also necessary which can be written as:

$$\varphi_{j,k}(x) = 2^{j/2}\varphi(2^j x - k) \quad j, k \in Z \tag{3}$$

The discrete form of wavelet transform of signal $f(x)$ at scale j can be written as:

$$\mathrm{Af}[j, i] = \sum_{n=1}^{N} f[n]\phi_{i,j}[n-i] \tag{4}$$

Thus, discrete wavelet decomposition of $f(x)$ can be given by:

$$f(x) = \sum_{k\in Z} C_{J,k}\Phi_{J,k}(x) + \sum_{i=1}^{J}\sum_{k\in Z} D_{i,J}\Psi_{i,k}(x) \tag{5}$$

$\{C_{J,k}\}$ is low-frequency decomposition coefficients set, that is, the coefficients of scale-functions. $\{D_{j,k}\}$ is high-frequency decomposition coefficients set, that is, coefficients of wavelet-functions.

2.2. Hilbert–Huang transform theory

Hilbert–Huang transform (HHT) [25], consisting of empirical mode decomposition and Hilbert transform, is an adaptive data analysis method, which has been widely used in signal processing. The technique works through performing EMD on signals. The signals can be decomposed into a set of complete and almost orthogonal components named IMF, which are almost monocomponent. Hilbert transform is carried out for those obtained IMFs, so we can get their instantaneous frequency and a full energy-frequency-time distribution of the signals.

2.2.1. Hilbert transform theory

Hilbert transform (HT), a well-known signal analysis method, is essentially defined as the convolution of signal $x(t)$ with $1/t$ and it can emphasize the local properties of $x(t)$ as follows:

$$y(t) = \frac{P}{\pi}\int_{-\infty}^{+\infty}\frac{x(\tau)}{t-\tau}d\tau \tag{6}$$

where P is the Cauchy principal value. Coupling the $x(t)$ and $y(t)$, the analytic signal $z(t)$ of $x(t)$ can be obtained which is given by

$$z(t) = x(t) + \mathrm{i}y(t) = a(t)e^{i\varphi(t)}, \tag{7}$$

where

$$a(t) = [x^2(t) + y^2(t)]^{1/2}, \quad \varphi(t) = \arctan(y(t)/x(t)). \tag{8}$$

$a(t)$ is the instantaneous amplitude of $x(t)$, which can reflect how the energy of the $x(t)$ varies with time, and $\varphi(t)$ is the instantaneous phase of $x(t)$.

One important property of the Hilbert transform is that if the signal $x(t)$ is monocomponent, so that the physical meaning of time derivative of instantaneous phase $\varphi(t)$ would be the instantaneous frequency $\omega(t)$ of signal $x(t)$. The instantaneous frequency equation is given by

$$\omega(t) = \frac{d\varphi(t)}{\mathrm{dt}} \tag{9}$$

2.2.2. Ensemble empirical mode decomposition (EEMD)

EEMD can solve the problem of mode mixing problem in EMD well [17]. It defines the true IMF components as the mean of an ensemble of trials. Each trial consists of the decomposition results of the signal plus a white noise of finite amplitude [26].

The EEMD algorithm can be given as follows.

(1) Initialize the number of ensemble M, the amplitude of the added white noise, and $m = 1$.
(2) Perform the mth trial on the signal added white noise.
   (a) Add a white noise series with the given amplitude to the investigated signal
   $$x_m(t) = x(t) + n_m(t) \tag{10}$$
   where $n_m(t)$ indicates the mth added white noise series, and $x_m(t)$ represents the noise-added signal of the mth trial.
   (b) Decompose the noise-added signal $x_m(t)$ into IMFs ($c_{i,m}$, $i = 1, 2, \ldots, I$), where $c_{i,m}$ denotes the ith IMF of the mth trial, and I is the number of IMFs.
   (c) If $m < M$ then go to step (a) with $m = m + 1$. Repeat steps (a) and (b) again and again, but with different white noise series each time.
(3) Calculate the ensemble mean $\bar{c}_i$ of the M trials for each IMF
$$\bar{c}_i = 1M\sum_{m=1}^{M} c_{i,m},\ i = 1, 2, \ldots, I, \quad m = 1, 2, \ldots, M \tag{11}$$
(4) Report the mean $\bar{c}_i$ ($i = 1, 2,$ ldots, I) of each of the I IMFs as the final IMFs.

3. Wavelet denoising with compensation of loss

3.1. Transfer function

Gaussian filter has been widely used in machined roughness measurement. It is a linear contour filter of the continuous weighting function defined by the equation $s(x)$ [27]:

$$s(x) = \frac{1}{\lambda_c}\exp\left[-\pi\left(\frac{x}{\alpha\lambda_c}\right)^2\right] \tag{12}$$

with x being the distance from the centre of the weighing function, λ_c the cut-off wavelength of the filter and α a constant value, defined by

$$\alpha = \sqrt{\frac{\log 2}{\pi}} = 0.4697\cdots \tag{13}$$

As the measured profile is usually given only at equidistant discrete points $x_k = k\Delta x$, the discrete representation of the Gaussian filter

$$s_k = \frac{\Delta x}{\alpha\lambda_c}\exp\left[-\pi\left(\frac{k\Delta x}{\alpha\lambda_c}\right)^2\right] \tag{14}$$

must be used, which is a good approximation of the continuous weighing function (12), as long as Δx is sufficiently small.

The transfer function of Gaussian filter can be calculated from a weighing function with Fourier transform.

$$H(\omega) = \frac{1}{2\pi}\int_{-\infty}^{+\infty} s(x)e^{-j\omega x}\mathrm{dx} = \exp\left[-\pi\left(\frac{a\omega}{\omega_c}\right)^2\right] \tag{15}$$

Wavelet filters, like Gaussian filters, are linear contour filters. The discrete form of wavelet transform of signal $f(x)$ at scale j can be written as:

$$\mathrm{Wf}[j, i] = \sum_{n=1}^{N} f[n]\psi[n-i] \tag{16}$$

The base function $\psi[n-i]$ in wavelet transform is also the weighting function. The transfer function of wavelet filter can be calculated from a base function with Fourier transform.

$$H(\omega) = F(\psi[n-i]) \tag{17}$$

3.2. Compensation using transfer function

For machined surface topography, wavelet transformation technique is applied for denoising firstly. However, while the surface noise is removed, some of the actual surface features are removed too. In order to obtain more accurate surface quality characteristics, it need to be compensated in the second step. The transfer function is needed in which instantaneous frequency is calculated by Hilbert transform. The coefficients of the transfer function are adjusted by improving the passing rate of real signals and lowering the passing rate of noise. However, using the Hilbert-transform to calculate the instantaneous frequency requires that the signal is monocomponent, so that the EEMD is needed before Hilbert-transform to decompose the denoising signal into several monocomponent layers. The correlation coefficient between each layer and the denoising signal is used to determine the IMFs to be retained. The wavelet denoising with compensation of loss (WDCL) process can be given as follows:

(1) Input original signal $x(t)$ and use wavelet filter to denoise the original signal to get the output signal $x_1(t)$.

(2)

(a) Use EEMD to decompose $x_1(t)$ into several IMFs (c_i, $i = 1, 2...n$).

(b) Use a threshold [28] which is dependent on the correlation coefficients between each layer and the denoising signal to determine the IMFs to be retained:

$$\rho_i = \frac{\mathrm{cov}(c_i, x_1)}{\sqrt{\mathrm{Var}(c_i)}\sqrt{\mathrm{Var}(x_1)}}, \quad i = 1, 2, \ldots, n \tag{18}$$

$$\rho_{\mathrm{th}} = \frac{\max(\rho_i)}{10\times\max(\rho_i) - 3}, \quad i = 1, 2, \ldots, n \tag{19}$$

where ρ_{th} is the threshold, ρ_i is the correlation coefficient of the ith IMF with the original signal, and n is the total number of IMFs; $\max(\rho_i)$ is the maximum correlation coefficient observed. The selection criterion for IMFs is given as follows: If $\rho_i \geq \rho_{th}$, then keep the ith IMF, else eliminate the ith IMF and add it to the residue.

(3) For those retained IMFs, calculate their instantaneous frequency by HT respectively.

$$\varphi_i(t) = \arctan\left(\frac{y_i(t)}{x_i(t)}\right), \quad \omega_i(t) = \frac{d\varphi_i(t)}{\mathrm{dt}} \; i = 1, 2, \ldots, J \tag{20}$$

where $y(t)$ is calculated by (6).

(4)

(a) As can be seen from the transform equation above, wavelet transform is essentially a discrete convolution form.

$$\mathrm{Wf}[j, i] = \sum_{n=1}^{N} f[n]\psi[n-i] \quad i = 1, 2, \ldots, J \tag{21}$$

According to the time-domain convolution theorem: the convolution integral of the two functions in the time domain corresponds to the product of the spectra of the two functions in the frequency domain:

$$f_1(t)f_2(t) \leftrightarrow F_1(\mathrm{jw})F_2(\mathrm{jw}) \tag{22}$$

After Fourier transform, the wavelet transform (21) becomes:

$$W_i = H_i Z_i \quad i = 1, 2, \ldots, J \tag{23}$$

where H is the Fourier transform of weighting function,

(b) Substitute the ω_i (20) into the equation (17), we can get the pass rate of each instantaneous frequency $H_i(\omega_i)$. For wavelet filter, it could delete noise and retain real surface feature. Thus a smaller $H_i(\omega_i)$ value indicates that the frequency is noise component which should be reduced further. While a larger $H_i(\omega_i)$ value indicates that the frequency is real surface feature component which should be enhanced further. $H_{1,i}(\omega_i)$ is the adjusted $H_i(\omega)$.

(c) Substitute $H_{1,i}(\omega)$ into formula (23), we can get a new output:

$$Z_{1,i} = W_i H_{1,i} \quad i = 1, 2, \ldots, J \tag{24}$$

(d) Through inverse Fourier transform (iFFT) we can get the signal after compensation and further noise reduction:

$$x_{c,i}(t) = \mathrm{iFFT}(Z_{1,i}(\omega_i)) \quad i = 1, 2, \ldots, J \tag{25}$$

(5) The compensated signal of each retained IMF is added to the final compensated signal $x_c(t)$:

$$x_c(t) = \sum_{i=1}^{J} x_{c,i}(t) \tag{26}$$

For the noise signal $x(t)$, the denoising signal $x_1(t)$ and the compensated signal $x_c(t)$, their signal-to-noise ratio (SNR) and energy are compared respectively.

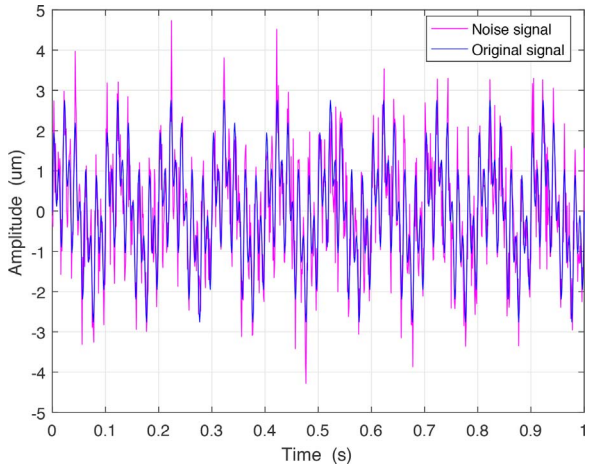

Fig. 1. Original signal and noise signal.

4. Applications to the test of machined surface topography

4.1. Simulation experiment

Machined surface topography contains complex frequency components, and it is often contaminated with heavy noise. These components contain useful information to extract the information needed to provide process feedback and trace errors of machine. This WDCL technology can be applied to test the machined surface topography. The denoising method based on Gaussian filtering is used to compare with WDCL.

Case 1: A test signal was given to show that WDCL could compensate energy loss and remove noise further. The original signal was $x_0 = \sin(2pi \cdot 10t) + \sin(2pi \cdot 50t) + \sin(2pi \cdot 100t)$. It was added to the Gaussian white noise with a signal to noise ratio of 5. The signal is shown in Fig. 1.

The cutoff wavelength of Gaussian filter is 8 μm, and Haar wavelet basis is used for 6-layer Wavelet decomposition. The spectrum of the noiseless original signal x_0 and the denoising signal x_1 are shown in Figs. 2 and 3 .

As we can see from Figs. 2 and 3, the original signal contains 3 frequency components 10 Hz, 50 Hz and 100 Hz. After denoising, energy loss occurred to the real frequency components of the original signal. Fig. 4 shows the IMFs we get after EEMD.

As is shown in Table 1, these IMFs' correlation coefficients with denoising signal were calculated. The values were arranged from large to small and the larger ones were picked out as the retained IMFs according to Eq. (19).

According to the process of WDCL, the instantaneous frequency of each point of the retained IMFs were calculated and put into transfer function. The transfer function were adjusted to get the compensated signal. The energy compensation effect of spectrum of the signal is shown in Fig. 5.

As we can see, energy loss occurred to the denoising signal. After EEMD decomposition, the spectrum of the signal reconstructed by the retained IMFs almost equal to the denoising signal. After compensation, the noise amplitude is still the same level as the denoising signal, but the energy of real frequency component is compensated in some extent.

In the end, the signal-to-noise ratio (SNR) and energy are used to measure the characteristics of the signal. The SNR of the noise signal, the denoising signals and the compensated signal are shown in Table 2. Table 3 shows their energy.

As we can see from tables above, energy loss after denoising is large, while the compensated signal can well make amend for it, which make it closer to the original signal. Besides, the SNR of the compensated signal is further improved. The larger of SNR, the better the de-noising effect is. It can be seen that the new method can achieve a good noise reduction effect, while reducing the energy loss compared with traditional denoising method based on Gaussian filtering.

The original signal, the noise signal, the wavelet denoising signal and the compensated signal are presented in Fig. 6. The original signal, the noise signal and the Gaussian denoising signal are shown in Fig. 7.

Case 2: In order to prove the effectiveness of the WDCL method, another test signal shown in Fig. 8 was analysed. The signal was

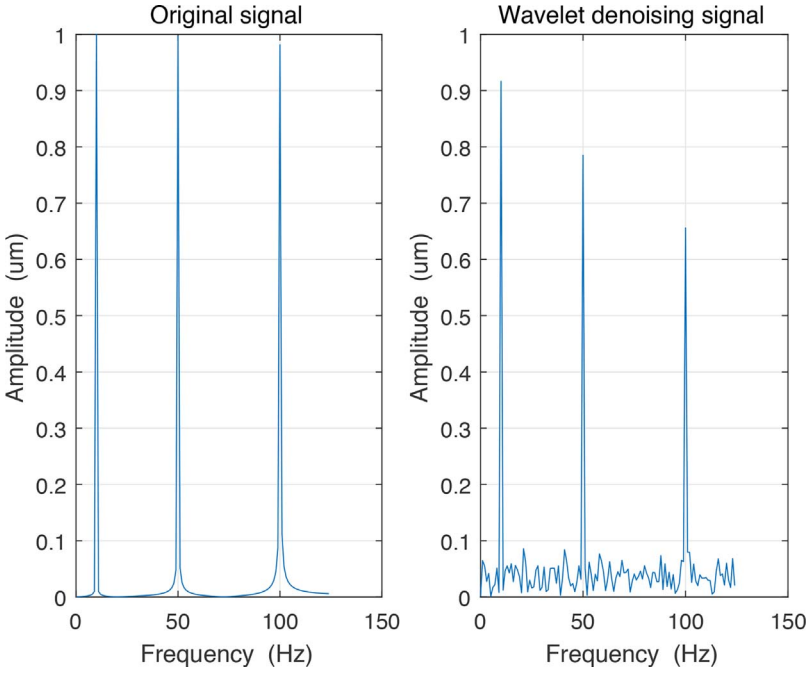

Fig. 2. Spectrum of original signal x_0 (left) and wavelet denoising signal x_1 (right).

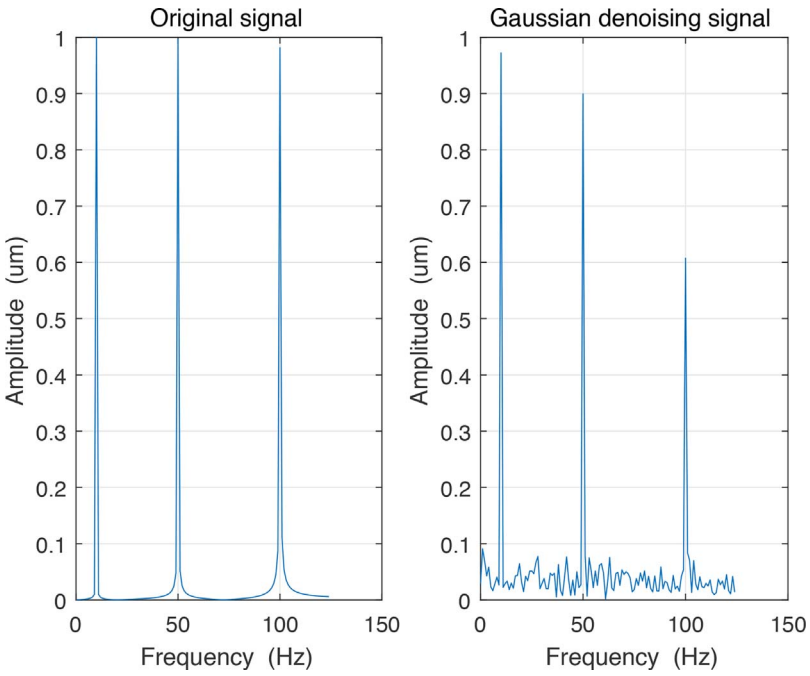

Fig. 3. Spectrum of original signal x_0 (left) and Gaussian denoising signal x_1 (right).

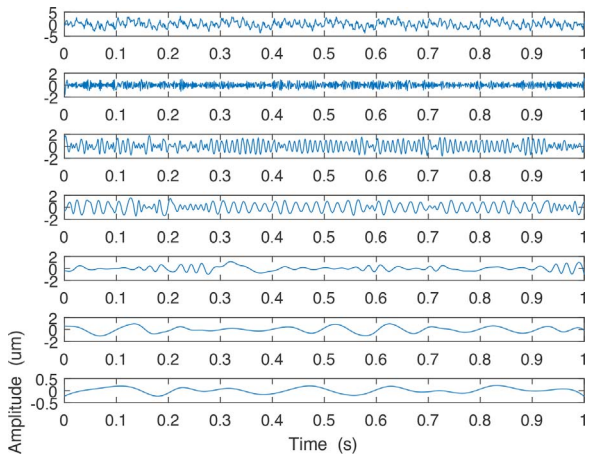

Fig. 4. Applying EEMD to denoising signal x_1.

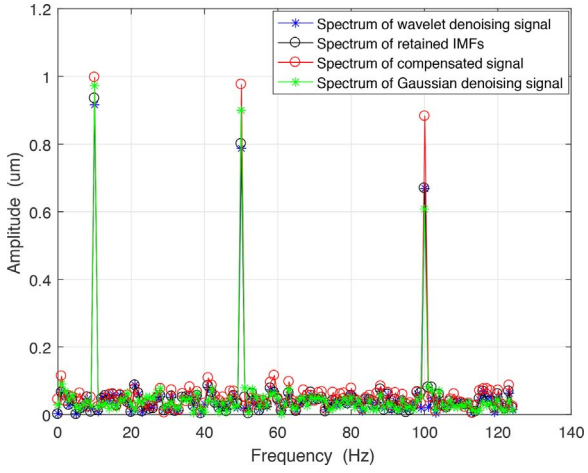

Fig. 5. Spectrum of denoising signals, retained IMFs and compensated signal.

Table 1
Correlation coefficient between each IMF and denoising signal.

EEMD	IMF1	IMF2	IMF3	IMF4	IMF5	IMF6	IMF7
Value	0.0882	0.4845	0.3991	0.1305	0.2948	0.025	0.012

generated by simulation and it was added on the white noise with a SNR of 5.

DC shift is removed first. The cutoff wavelength of Gaussian filter is 0.08 mm, and Haar wavelet basis is used for 5-layer Wavelet decomposition. The spectrum of noiseless original signal x_0 and denoising signals x_1 are shown in Figs. 9 and 10 .

As we can see from pictures above, the energy of the low frequency components have a different degree of loss after different methods of noise reduction. The high frequency components of wavelet denoising signal are still retained while the high frequency components of

Table 2
SNR of 4 kinds of signals.

Signal	SNR
Noise signal	5.0043
Gaussian denoising signal	6.0794
Wavelet denoising signal	6.6257
Compensated signal	7.9128

Table 3
Energy comparison of each signal.

Signal	Energy
Noise signal	1948.4
Original signal	1500
Gaussian denoising signal	1169.3
Wavelet denoising signal	1200
Compensated signal	1536

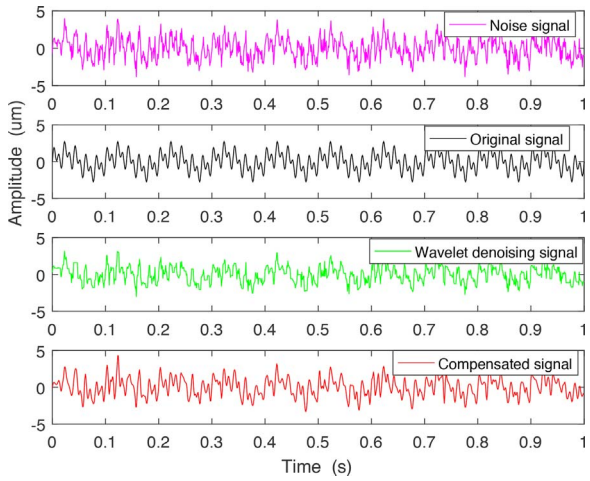

Fig. 6. Noise signal, original signal, wavelet denoising signal and compensated signal.

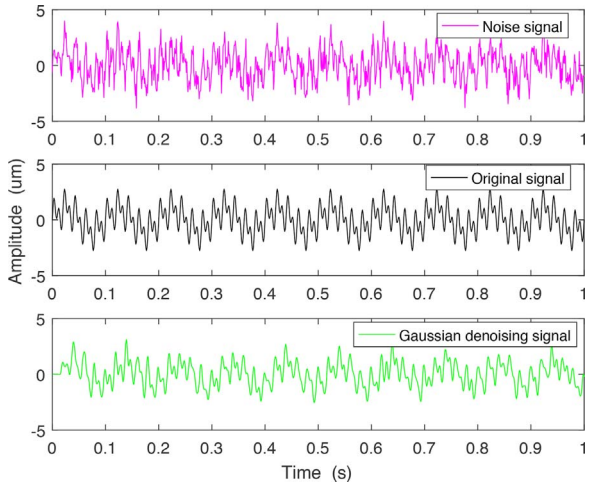

Fig. 7. Noise signal, original signal and Gaussian denoising signal.

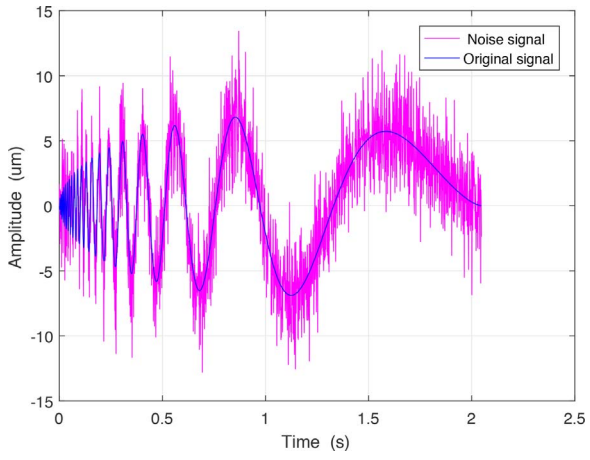

Fig. 8. Original signal and noise signal.

Gaussian denoising signal are directly removed. The calculation result of the EEMD decomposition process and the correlation coefficients of IMFs are no longer shown here.

According to the process of WDCL, the energy compensation effect of spectrum of the signal is shown in Fig. 11.

By WDCL we can get the energy which is closer to the real frequency component. The SNR and energy are used to measure the characteristics of signal which are shown in Tables 4 and 5 .

As we can see from tables above, the SNR of the compensated signal is further improved than the wavelet denoising signal while the energy of the compensated signal is closer to the original signal. Besides, compared with Gaussian noise reduction method, the SNR values show that both methods can achieve good denoising effect. However, the high frequency part of the signal is directly cut off causing the loss of the true component in high frequency domain, which is not conducive to the separation and extraction of surface features. But the WDCL method could not only denoise signal in the entire frequency domain, but also perform energy compensation after noise reduction which achieves a better denoising effect than Gaussian denoising method.

By using iFFT the compensated signal was obtained. The original signal, the noise signal, the denoising signals and the compensated signal are shown in Figs. 12 and 13 .

As can be seen from picture above, Gaussian noise reduction method results in loss of true high frequency components.

4.2. Test of S test-piece surface topography

A S test-piece [29] is an important workpiece in mechanical field which is shown in Fig. 14. S-type specimen is a newly proposed test piece to verify the dynamic performance of the machine tool which is obtained by performing flank milling operation on it. By cutting S-type specimen to a certain extent, the dynamic performance of five-axis CNC machine tools can be reflected. However, the surface topography obtained from S-type specimen is often immersed in heavy noise. The noise could be generated by aperiodic stochastic vibration which is caused by random factors during the cutting process and distribute throughout the entire frequency domain. Therefore, the surface features are denoised first. Surface profiler, 2300A-R with sample step of 1 μm, has a measuring range of 1200 μm and a resolution of 18 nm/1200 μm, was applied to measure the S-type specimen surface quality. The measurement area is shown in Fig. 14. The signal length is 500, the sampling interval is 1 μm and the sampling frequency is 1000 Hz. The original signal and denoising signals are shown in Figs. 15 and 16 .

Noise signal is the real signal with noise that we measured from the surface of the S-type specimen. Form error was removed first and noise reduction was carried out by wavelet filter and Gaussian filter. The cutoff wavelength of Gaussian filter is 8 μm, and Haar wavelet basis is used for 6-layer wavelet decomposition. The spectrum of the noise signal and the denoising signals are shown in Fig. 17. The wavelength is inversely proportional to the frequency. As we can see, the high-frequency component of signal is still retained after wavelet noise reduction, and noise reduction was also carried out in the low-frequency component. Since the Gaussian filter is low-pass filter, so that there is almost no noise reduction for low frequency components, but the higher frequency components is directly eliminated.

According to the process of WDCL, the compensated signal was obtained. The loss of the low-frequency component of wavelet denoising was compensated. The spectrum of the noise signal, the compensated signal and the denoising signals are compared in Fig. 18. Table 6 shows their energy comparison.

As noise is generated by the random factors of the matching tool so that we could not get the original noiseless signal. SNR values are no longer shown here. As can be seen from the figure and table above, the energy of the compensated signal and the wavelet denoising signal are almost equal but the energy of the low frequency component of the compensated signal is higher than the wavelet denoising signal, so we could deduce that the residual noise in the high frequency part is

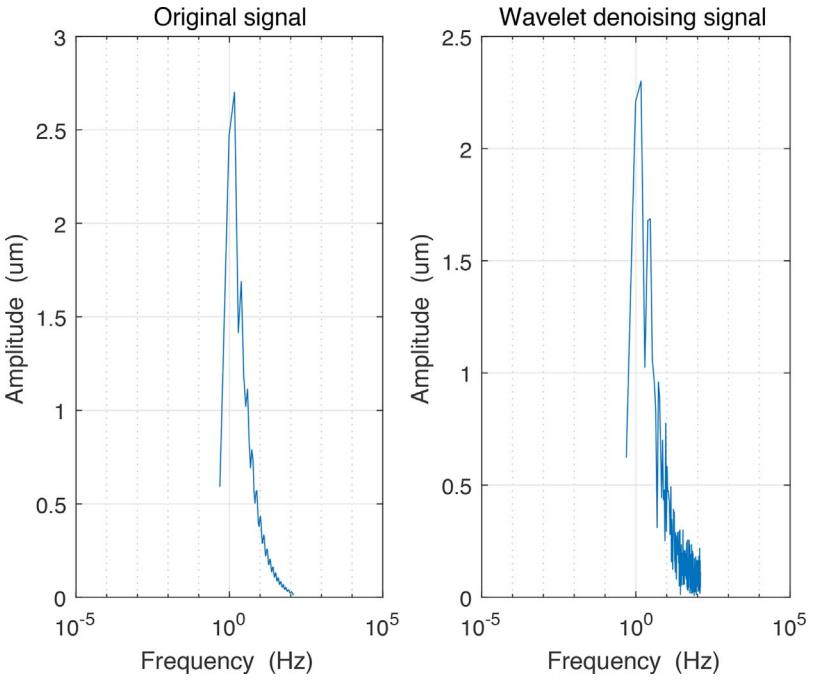

Fig. 9. Spectrum of original signal x_0 and denoising signal x_1.

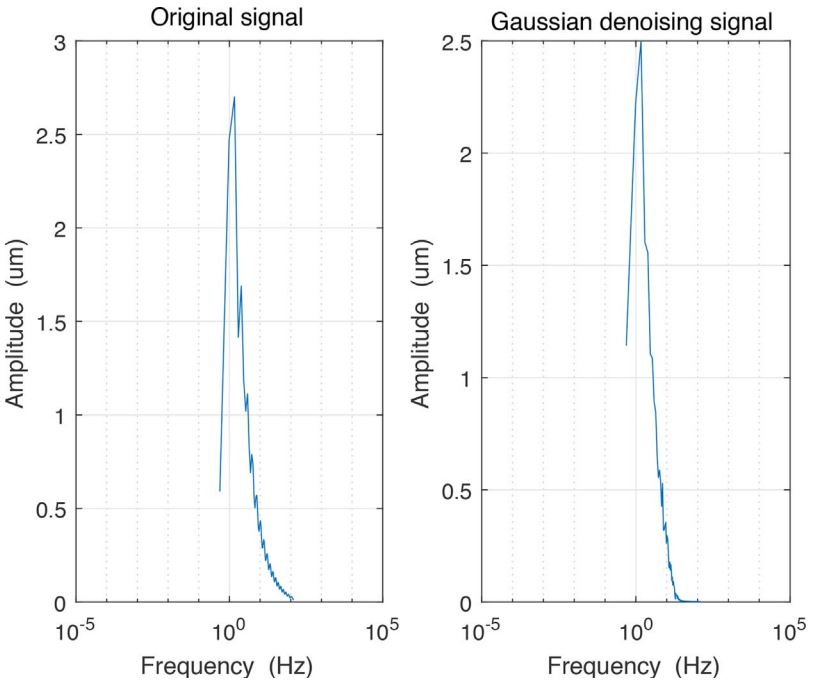

Fig. 10. Spectrum of original signal x_0 and denoising signal x_1.

reduced further, that is, the SNR is further improved. Besides, the SNR of the compensated signal is also improved compared with the signal of Gaussian noise reduction. In summary, the WDCL method can achieve a good noise reduction effect in the entire frequency-domain while compensating the energy loss effectively. These signals are shown in Fig. 19.

5. Discussion and conclusion

To solve the problem of energy loss caused by wavelet denoising, an improved signal determination method called WDCL was proposed in this paper. The energy compensation was mainly carried out by the adjustment of the transfer function. To get the transfer function, we need the Fourier transform of wavelet base function and the instantaneous frequency of each point as the independent variable of the transfer function. First, the EEMD was used to decompose the denoising signal. Second, for each IMF we selected, Hilbert transform was calculated to get the instantaneous frequency of each point, thus transfer coefficient of each point was obtained. Finally, to get the adjusted transfer function, the coefficients of the high passing rate were increased and the coefficients of the low passing rate were reduced further. The compensated signal was obtained by multiplying the adjusted transfer function and the denoising result.

The S test-piece was used to validate the capabilities of the proposed method. The applications to machined surface topography show that the proposed method can effectively compensate for energy loss caused

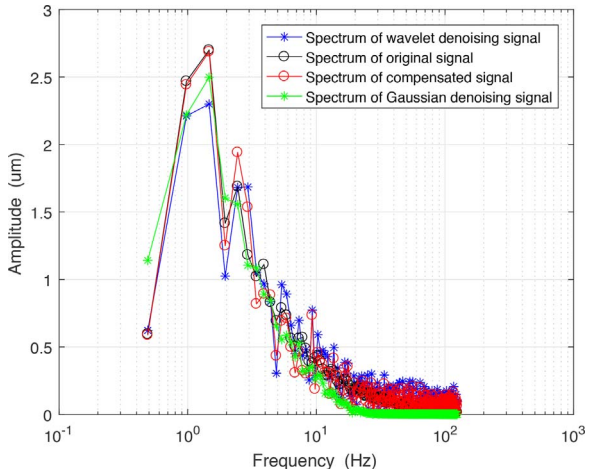

Fig. 11. Spectrum of original signal, denoising signals and compensated signal.

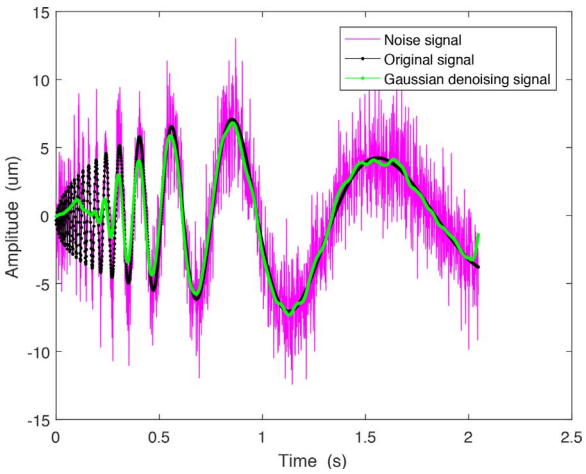

Fig. 13. Noise signal, original signal and Gaussian denoising signal.

Table 4
SNR of 4 kinds of signals.

Signal	SNR
Noise signal	5.0021
Gaussian denoising signal	9.2238
Wavelet denoising signal	7.8744
Compensated signal	10.4233

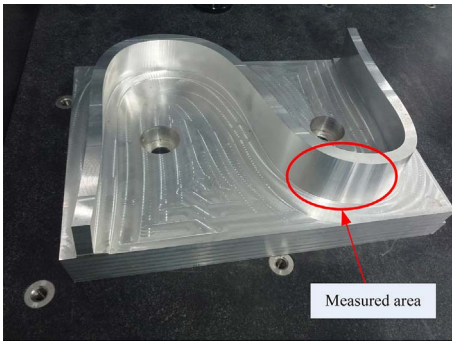

Fig. 14. S test-piece and the measured area.

Table 5
Energy comparison of each signal.

Signal	Energy
Noise signal	4.0254e+04
Original signal	2.9956e+04
Gaussian denoising signal	2.5039e+04
Wavelet denoising signal	2.4328e+04
Compensated signal	2.9570e+04

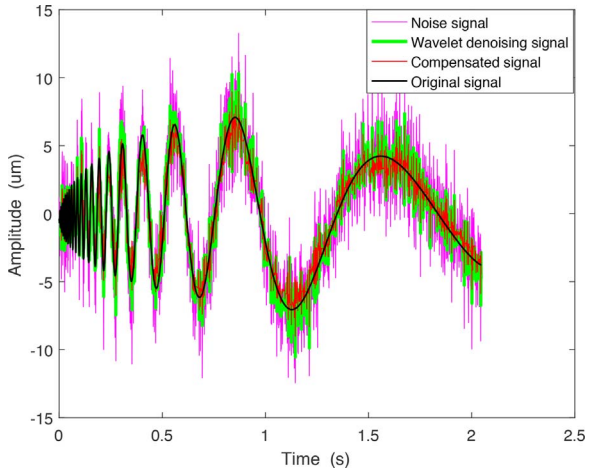

Fig. 12. Noise signal, original signal, wavelet denoising signal and compensated signal.

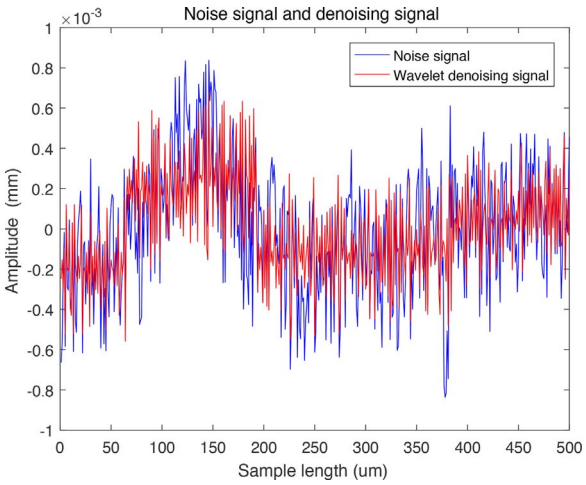

Fig. 15. Noise signal and wavelet denoising signal.

by denoising. Compared to traditional denoising method, the wavelet denoising method could reduce noise in the entire frequency-domain and the compensation method could compensate the energy loss at the same time. Thus, the WDCL could achieve good denoising effect while reducing energy loss. The analysed results demonstrate that the proposed method is an effective approach to denoise signals and analyse surface topography quality.

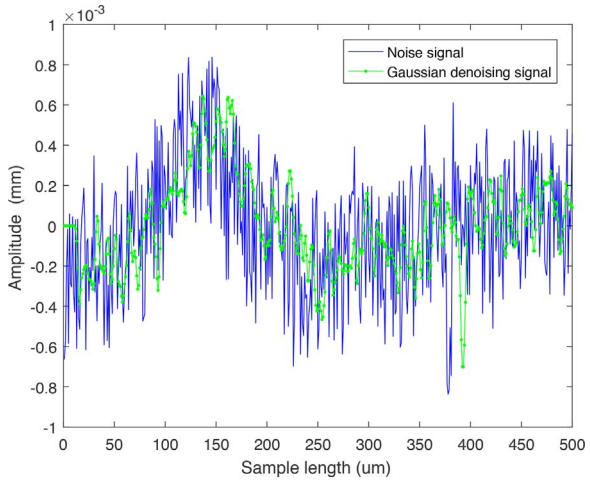

Fig. 16. Noise signal and Gaussian denoising signal.

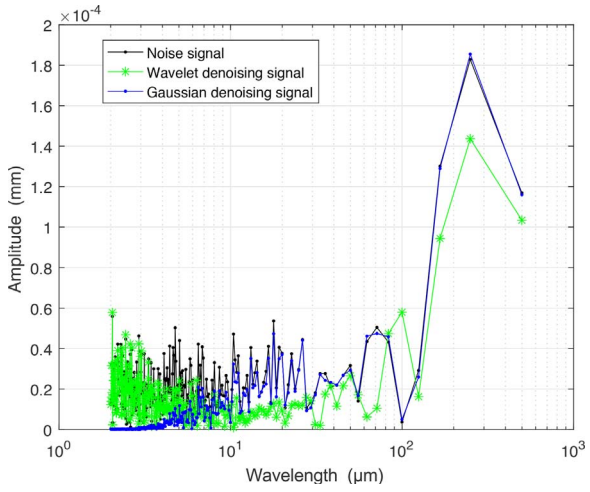

Fig. 17. Spectrum of noise signal and denoising signals.

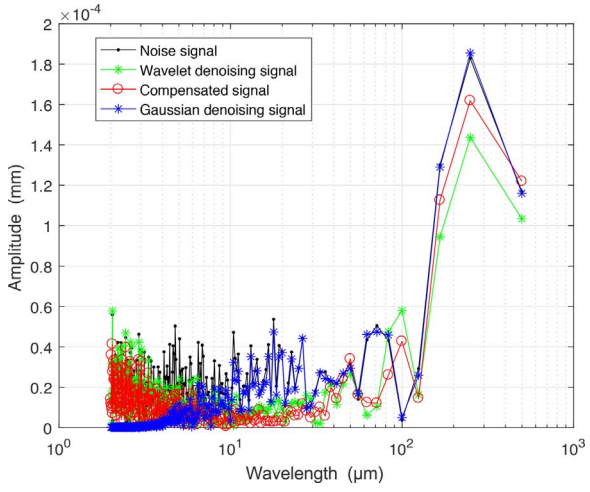

Fig. 18. Spectrum of noise signal, denoising signals and compensated signal.

Table 6
Energy comparison of each signal.

Signal	Energy
Noise signal	52.7996
Gaussian denoising signal	25.4137
Wavelet denoising signal	29.0236
Compensated signal	28.8098

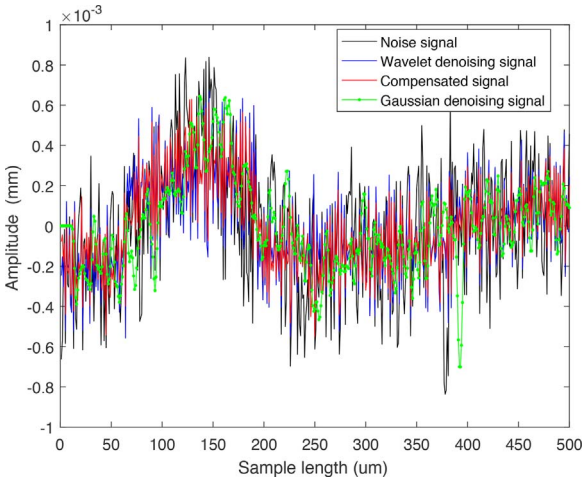

Fig. 19. Noise signal, denoising signals and compensated signal.

Acknowledgements

This work is supported by National Natural Science Foundation of China (No. 51675378) and the Natural Science Foundation of Tianjin (No. 16JCYBJC15900).

References

[1] Chen D, Zhou S, Dong L, Fan J. An investigation into error source identification of machine tools based on time–frequency feature extraction. Shock Vibr 2016;2016:1–10.
[2] Guo ZP, Song ZY, Shi RB. Error source identification of machining accuracy of five-axis linkage CNC machine tools. Adv Mater Res 2014;846-847:34–9.
[3] Wang H, Chen J, Dong G. Feature extraction of rolling bearing's early weak fault based on EEMD and tunable q-factor wavelet transform. Mech Syst Signal Process 2014;48(1–2):103–19.
[4] Kiela K, Navickas R. A method for continuous tuning of MOSFET-RC filters with extended control range. J Electr Eng 2016;67(6):449–53.
[5] Janecki D. Gaussian filters with profile extrapolation. Precis Eng 2011;35(4):602–6.
[6] Janecki D, Cedro L, Zwierzchowski J. Separation of non-periodic and periodic 2d profile features using b-spline functions. Metrol Meas Syst 2015;22(2):289–302.
[7] Huang NE, Shen Z, Long SR, Wu MC, Shih HH, Zheng Q, Huang NE, et al. The empirical mode decomposition and the Hilbert spectrum for nonlinear and non-stationary time series analysis. Proc R Soc A Math Phys Eng Sci 1998;454(1971):903–95.
[8] Kumar U, Yadav I, Kumari S, Kumari K, Ranjan N, Kesharwani RK, et al. Defect identification in friction stir welding using discrete wavelet analysis. Adv Eng Softw 2015;85(C):43–50.
[9] Donoho DL, Johnstone IM. Ideal spatial adaptation by wavelet shrinkage. Biometrika 1994;81(3):425–55.
[10] Cai TT, Silverman BW. Incorporating information on neighboring coefficients into wavelet estimation. Sankhya 1999;63(2):127–48.
[11] Peng Z, Chu F. Vibration signal analysis and feature extraction based on reassigned wavelet scalogram. J Sound Vibr 2002;253(5):1087–100.
[12] Huang NE, Shen Z, Long SR. A new view of nonlinear water waves: the Hilbert spectrum. Fluid Mech 1999;31(31):417–57.
[13] Montesinosa ME, Pérezb OC. Hilbert–Huang analysis of BWR neutron detector signals: application to DR calculation and to corrupted signal analysis. Ann Nucl Energy 2003;30(6):715–27.
[14] Náprstek J, Fischer C. Non-stationary response of structures excited by random seismic processes with time variable frequency content. Soil Dyn Earthquake Eng 2002;22(22):1143–50.

[15] Peng ZK, Tse PW, Chu FL. A comparison study of improved Hilbert–Huang transform and wavelet transform: application to fault diagnosis for rolling bearing. Mech Syst Signal Process 2005;19(5):974–88.
[16] Zhang F, Yang J, Zhang T, Yan Y. Surface topography separation based on wavelet reconstruction and empirical mode decomposition. ASME 2015 international manufacturing science and engineering conference. 2015.
[17] Wu Z, Huang NE. Ensemble empirical mode decomposition: a noise-assisted data analysis method. Adv Adapt Data Anal 2011;1(1):1–41.
[18] Dybala J, Zimroz R. Rolling bearing diagnosing method based on empirical mode decomposition of machine vibration signal. Appl Acoust 2014;77(3):195–203.
[19] Meng L, Xiang J, Wang Y, Jiang Y, Gao H. A hybrid fault diagnosis method using morphological filter-translation invariant wavelet and improved ensemble empirical mode decomposition. Mech Syst Signal Process 2015;50-51:101–15.
[20] Flores-Bahamonde F, Valderrama-Blavi H, Bosque-Moncusi JM, García G. Using the sliding-mode control approach for analysis and design of the boost inverter. IET Power Electron 2016;9(8):1625–34.
[21] Vidal A, Freijedo FD, Yepes AG, Fernandez-Comesana P. Assessment and optimization of the transient response of proportional-resonant current controllers for distributed power generation systems. Ind Electron IEEE Trans 2013;60(4):1367–83.
[22] Battista BM, Knapp C, Mcgee T, Goebel V. Application of the empirical mode decomposition and Hilbert–Huang transform to seismic reflection data. Geophysics 2007;72(2):H29–37.
[23] Chai X, Wang S, Yuan S, Zhao J, Sun L, Wei X. Sparse reflectivity inversion for nonstationary seismic data. Geophysics 2014;79(3):V93–105.
[24] Wang J, Cheng J, Lu T, Zou Y. Spectrum whitening in time–frequency domain for deep part coal resource seismic exploration. International conference on remote sensing, environment and transportation engineering. 2011. p. 1594–7.
[25] Huang NE, Wu Z. A review on Hilbert–Huang transform: Method and its applications to geophysical studies. Rev Geophys 2008;46(2):2008.
[26] Lei Y, He Z, Zi Y. Application of the EEMD method to rotor fault diagnosis of rotating machinery. Mech Syst Signal Process 2009;23(4):1327–38.
[27] Krystek M. Measurement uncertainty propagation in the case of filtering in roughness measurement. Meas Sci Technol 2001;12(1):63–7.
[28] Ayenu-Prah A, Attoh-Okine N. A criterion for selecting relevant intrinsic mode functions in empirical mode decomposition. Adv Adapt Data Anal 2010;2(1):1–24.
[29] Wang W, Jiang Z, Tao W, Zhuang W. A new test part to identify performance of five-axis machine tool – Part I. Geometrical and kinematic characteristics of s part. Int J Adv Manuf Technol 2015;79(5):729–38.